# 21. MODELS OF WHITE DWARFS, RADIAL PULSATIONS AND VIBRATIONAL STABILITY

G. VAUCLAIR
*Institut d'Astrophysique de Paris, France*

## 1. Models of White Dwarfs

We have computed a set of models of white dwarfs. The equation of state is the Chandrasekhar (1939) one corrected by Salpeter (1961). It takes into account both the interactions between particles and the effect of non-zero temperature.

The models consist of an isothermal core with 50% of carbon and 50% of oxygen, surrounded by an envelope of population I composition with 70% of hydrogen and 3% of metals by mass. Nuclear energy is liberated by p-p reactions located in a shell at the edge of the isothermal core. Equilibrium models of various masses and luminosities have been built; Table I gives the values of their characteristic parameters. The central temperature-luminosity-mass relation for our models is compared with the Schatzman (1952) one for pure hydrogen envelopes (S), the Hubbard and Wagner (1970) one for Mg core and solar composition envelope models (HW) and the Van Horn (1970) one for carbons models (VH) (Figure 1). At high luminosities there is a sensible departure from the linear relation. Though our models are not evolutionary sequence ones, they fit very well with the sequences calculated by Vila (1966, 1967). The models studied here are of the type expected from the calculation of the evolution of some double systems (Lauterborn, 1970) after the white dwarfs have lost their very diluted envelopes.

## 2. Eigenvalues and Eigenfunctions of the Radial Pulsations

The eigenvalues and eigenfunctions of radial pulsations are calculated in the adiabatic assumption for the fundamental mode. We confirm that the eigenfunctions do not decrease very much through the white dwarfs. However, it is only for the more massive white dwarfs that the eigenfunction is constant; but for less massive models it decreases inward (Figure 2). No steep gradient are found in the envelopes. The periods vary in the range 3.8 sec for the 1.2 $M_\odot$ models to 18.5 sec for the 0.4 $M_\odot$ one. Our periods are compared with (1) the periods of Harper and Rose's (1969) zero temperature models, (2) the periods of Ostriker and Tassoul's (1969) non rotating white dwarfs models, and (3) the periods of Cohen *et al.* (1969) carbon models; the two first ones built up according to the Chandrasekhar equation of state, and the last one according to the same equation of state improved by Salpeter's corrections (Table II). The decrease of the periods is due to the improvement of both the equations of state and the adiabatic gradient.

*Luyten (ed.), White Dwarfs,* 145–154. 

https://doi.org/10.1017/S0074180900097205 Published online by Cambridge University Press

TABLE
Models of

| 1 | 2 | 3 | 4 | 5 | 6 | 7 | 8 |
|---|---|---|---|---|---|---|---|
| No. | $M/M_\odot$ | $R/R_\odot$ | $L/L_\odot$ | Log$g$ | Log$T_{\text{eff}}$ | $M_B$ | $T_c$ ($10^6$K) |
| 1 | 1.2 | $5.411 \times 10^{-3}$ | $8.5518 \times 10^{-3}$ | 9.050 | 4.3798 | 9.8898 | 9.4107 |
| 2 | 1.2 | $5.4663 \times 10^{-3}$ | $9.1305 \times 10^{-2}$ | 9.041 | 4.6347 | 7.3187 | 18.1631 |
| 3 | 1 | $8.0114 \times 10^{-3}$ | $1.0735 \times 10^{-1}$ | 8.63 | 4.5693 | 7.1429 | 17.9109 |
| 4 | 1 | $7.8694 \times 10^{-3}$ | $9.1288 \times 10^{-3}$ | 8.644 | 4.3056 | 9.8189 | 9.6652 |
| 5 | 0.8 | $1.0596 \times 10^{-2}$ | $2.0348 \times 10^{-1}$ | 8.293 | 4.5780 | 6.4486 | 19.0456 |
| 6 | 0.6 | $1.3997 \times 10^{-2}$ | $4.2644 \times 10^{-1}$ | 7.924 | 4.5979 | 5.6453 | 20.2989 |
| 7 | 0.6 | $1.2763 \times 10^{-2}$ | $2.1026 \times 10^{-3}$ | 7.994 | 4.0412 | 11.4131 | 6.6209 |
| 8 | 0.4 | $1.6942 \times 10^{-2}$ | $3.7687 \times 10^{-3}$ | 7.587 | 4.0430 | 10.7795 | 8.00 |

*Notes* – 1: number of the model; 2: mass in solar mass unit; 3: radius in solar radius unit; 4: luminosity in magnitude; 8: central temperature in million degree K; 9: central pressure in c.g.s.; 10: central density in g cm$^{-3}$; shell; 13: fraction of the radius occupied by the partially degenerate shell; 14: fraction of the radius occupied

The effect of the temperature is an increase of the radius and of the pulsation period. For instance, the first 0.6 $M_\odot$ model, number 7, with a central temperature of $6.6 \times 10^6$ K, has a radius of $8.96 \times 10^8$ cm and a period of 11.74 sec, and the second, number 6, with a central temperature of $20.10^6$ K has a radius of $9.72 \times 10^8$ cm and a period of 11.81 sec. When the temperature increases by 3 orders of magnitude,

TABLE II
Radial pulsation periods for white dwarfs

| $M/M_\odot$ | $P_{\text{sec}}$ [1] | $P_{\text{sec}}$ [2] | $P_{\text{sec}}$ [3] | This work No. | $P_{\text{sec}}$ | $\frac{\xi_s}{\xi_c}$ |
|---|---|---|---|---|---|---|
| 0.4 | 23.4 | 20.6 | 18.5 | 8 | 18.453 | 1.695 |
| 0.6 | 14.4 | 12.8 | 11.85 | 7 | 11.740 | 1.315 |
| | | | | 6 | 11.811 | 1.500 |
| 0.8 | 9 | 9 | 8.3 | 5 | 8.167 | 1.220 |
| 1.0 | 6.2 | 6.4 | 5.9 | 4 | 5.740 | 1.060 |
| | | | | 3 | 5.747 | 1.070 |
| 1.2 | 4 | 4.4 | 3.8 | 2 | 3.800 | 0.970 |
| | | | | 1 | 3.797 | 0.970 |

*Notes* – Eigenfunctions of radial pulsations of white dwarfs. For the masses given in the first column, the table gives the periods from Harper and Rose (1969) (1) Ostriker and Tassoul (1969) (2) Cohen *et al.* (1969) (3) in comparison with our results. The last columns give the number of the models, their periods and the ratio of the amplitudes of the eigenfunction at the surface and at the center.

I
white dwarfs

| 9 | 10 | 11 | 12 | 13 | 14 | 15 |
|---|---|---|---|---|---|---|
| $P_c$ cgs | $\varrho_c$ gr | $\eta_c$ | Non-isothermal shell (% of the radius) | partially degenerate shell % | H burning shell % | H content |
| $4.9318 \times 10^{25}$ | $1.8719 \times 10^{8}$ | 6585 | 3.77 | 1.39 | 2 | $3.79 \times 10^{-5}$ |
| $4.8915 \times 10^{25}$ | $1.8604 \times 10^{8}$ | 3398 | 4.08 | 3.1 | 1.77 | $2.0 \times 10^{-5}$ |
| $5.2990 \times 10^{24}$ | $3.7042 \times 10^{7}$ | 1175 | 6.18 | 5.62 | 2.49 | $7.5 \times 10^{-5}$ |
| $5.3389 \times 10^{24}$ | $3.7250 \times 10^{7}$ | 2185 | 5.15 | 2.67 | 2.95 | $9.38 \times 10^{-5}$ |
| $9.8262 \times 10^{23}$ | $1.1318 \times 10^{7}$ | 501 | 9.35 | 8.88 | 3.06 | $1.46 \times 10^{-4}$ |
| $1.9803 \times 10^{23}$ | $3.8218 \times 10^{6}$ | 228 | 15.2 | 14.22 | 3.87 | $3.45 \times 10^{-4}$ |
| $2.0192 \times 10^{23}$ | $3.8759 \times 10^{6}$ | 705 | 8.8 | 4.99 | 4.66 | $4.85 \times 10^{-4}$ |
| $3.3317 \times 10^{22}$ | $1.1957 \times 10^{6}$ | 266 | 15.7 | 12.32 | 6.8 | $1.2 \times 10^{-3}$ |

solar luminosity unit; 5: logarithm of the surface gravity; 6: logarithm of the effective temperature; 7: Bolometric
11: value of the parametre of degeneracy at the center; 12: fraction of the radius occupied by the non-isothermal
by the Hydrogen burning shell; 15: content in Hydrogen in fraction of total mass.

the radius increases by 8.5% and the period by 0.6%. This confirms the result of Hubbard and Wagner (1970) who find an increase of the period from 17.39 sec to 18.04 sec for a 0.43 $M_\odot$ model with a central temperature increasing from 0 K to $1.29 \times 10^7$ K ($10^{-2}$ $L_\odot$). The more the mass of the models decreases, the more this effect of the temperature on the period is sensible. The increase of the period is $5.2 \times 10^{-9}$ sec $K^{-1}$ for our 0.6 $M_\odot$ models, and $5 \times 10^{-8}$ sec $K^{-1}$ for the Hubbard and Wagner's 0.43 $M_\odot$ models.

## 3. Vibrational Stability

The vibrational stability is studied by evaluating the overall dissipation according to the method described by Ledoux and Walraven (1958).

Three mechanisms can amplify the oscillations: (a) the classical $\varkappa$-mechanism in the external He II ionization zone; (b) the driving due to an external source of energy; here, the hydrogen burning shell; and (c) the increase of the perturbation in luminosity outward in the central part of the isothermal core due to the relative variation of the opacity and adiabatic gradient in this very degenerate region.

The relative influence of the different shells on the overall instability is shown by the behaviour of the energy integral throughout the star:

$$E = \int_0^M \left(\frac{\delta T}{T}\right)_a \delta\left(\varepsilon - \frac{1}{\varrho} \operatorname{div} F\right)_a \mathrm{d}m$$

https://doi.org/10.1017/S0074180900097205 Published online by Cambridge University Press

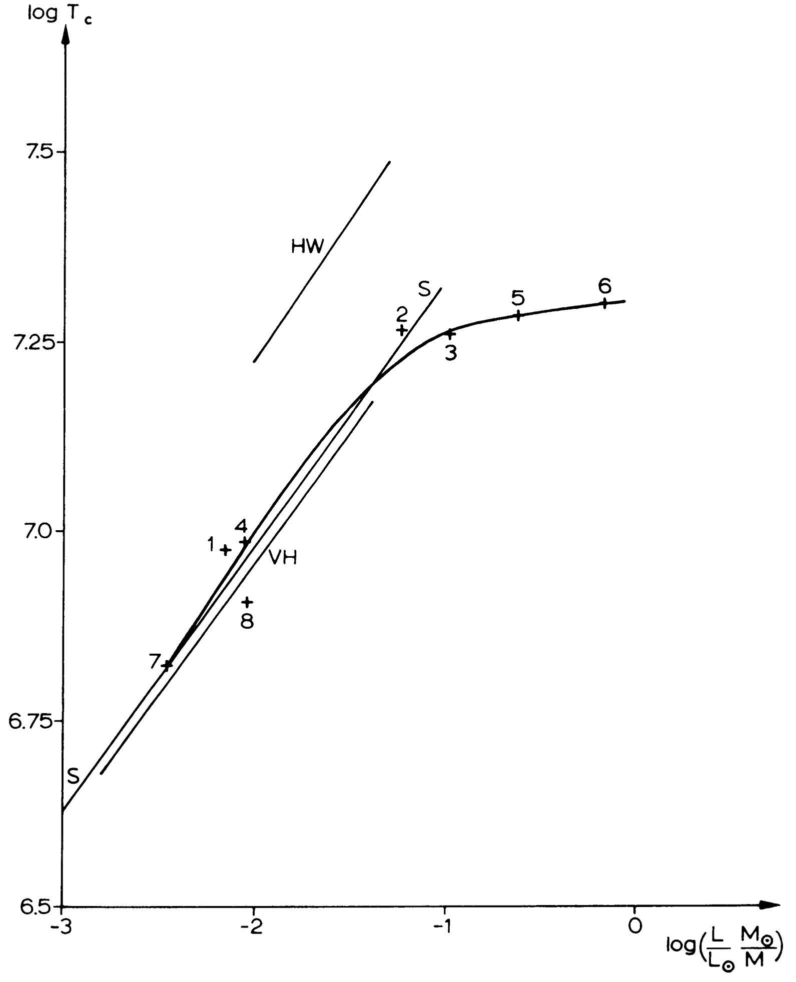


Fig. 1. Log $T_c$ vs $\log(L/L_{\odot} \cdot M_{\odot}/M)$ for the eight models compared with Schatzman's (S), van Horn's (VH), and Hubbard-Wagner's (HW) relationships.

Figure 3 shows in model 1 the influence on the driving of the oscillations, due to the H and He I ionization zone, and to the He II one. The He II ionization zone plays the most important role. At the edge of the isothermal core, the hydrogen burning shell provides a driving of the same order of magnitude as the He II ionization one. The isothermal core itself begins to damp the pulsations but it amplifies them in its innermost central part. The $x$-mechanism alone is not able to trigger the instability. The behaviour of the energy integral in model 4 is analogous.

In model 8 (Figure 4) (and also model 7) the instability is mainly due to mechanism $a$. The excitation due to the H burning shell is indeed three times smaller than the excitation due to the ionization zone, and without this H burning shell the models would be unstable by $x$-mechanism alone.

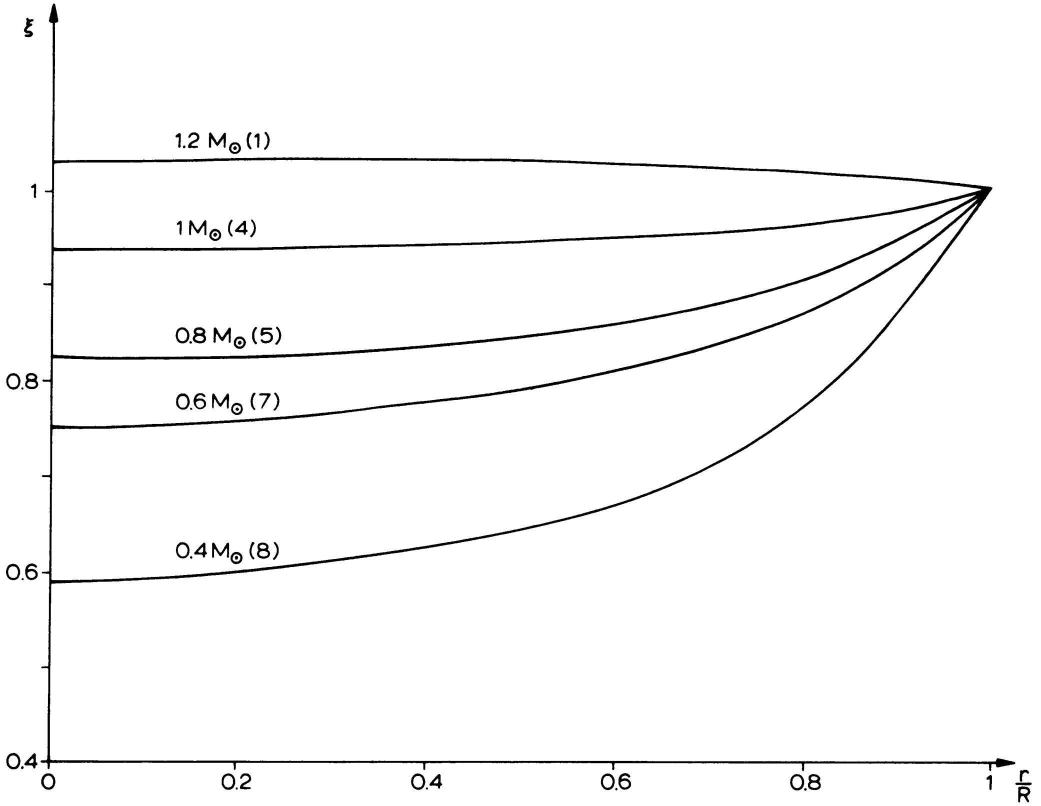


Fig. 2. Eigenfunction in different mass models vs the relative radius.

TABLE III

| No. | $T$ (yr) |
|---|---|
| 1 | 6.35 (10) |
| 2 | 2.36 (8) |
| 3 | 1.46 (8) |
| 4 | 1.835 (10) |
| 5 | 3.18 (7) |
| 6 | 5.875 (6) |
| 7 | 9.68 (9) |
| 8 | 1.42 (9) |

*Note* – In the first column: the number of the model; in the second one the amplification rate, the number in parenthesis is the power of ten.

https://doi.org/10.1017/S0074180900097205 Published online by Cambridge University Press

On the contrary in model 5 (Figure 5) (and also models 2, 3 and 6) the amplification is caused predominantly by the mechanism *b*. The part of the isothermal core becomes negligible.

## 4. Remark

In this set of models of white dwarfs, the energy source considered is the hydrogen burning shell located at the edge of the isothermal core. In an improved treatment we should include the cooling of the degenerate core. But when this cooling is taken

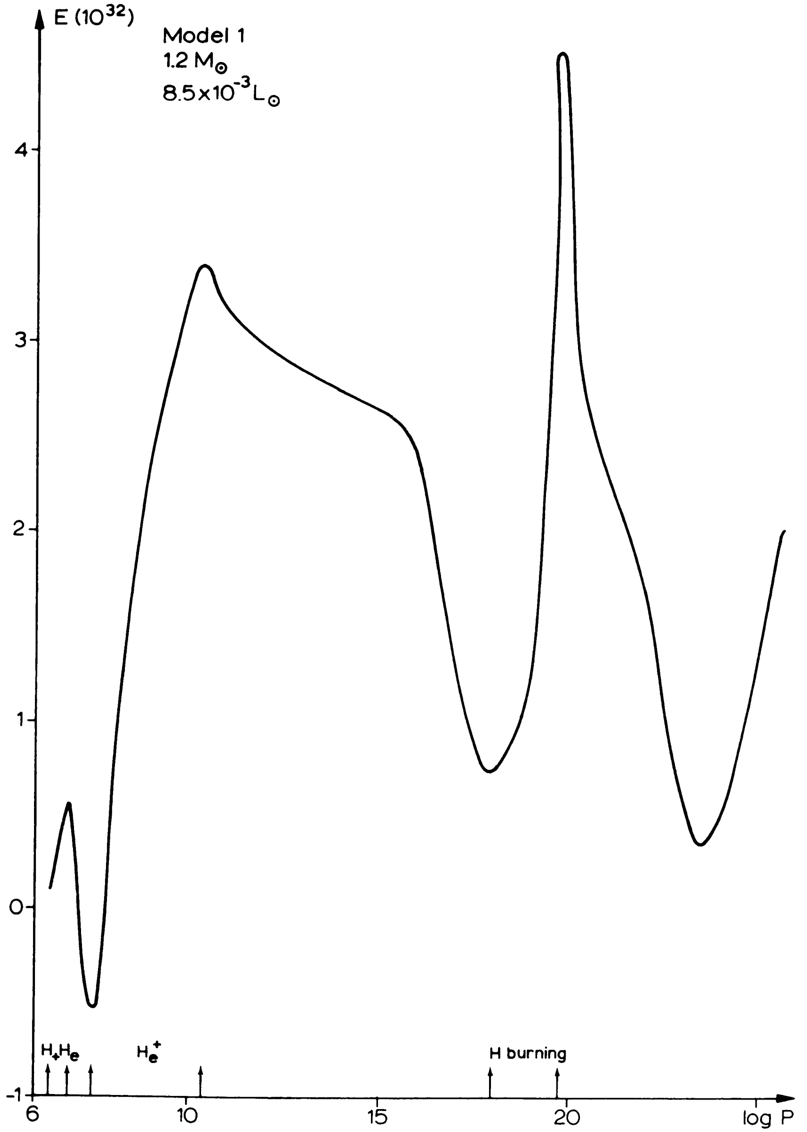


Fig. 3. The energy integral vs the logarithm of the pressure in the model 1.

https://doi.org/10.1017/S0074180900097205 Published online by Cambridge University Press

into account, the structure of the core is not modified because the electronic conductibility in a degenerate gas keeps the temperature gradient very small such as we may consider the core as isothermal.

For a model with a given luminosity, the contribution of the hydrogen burning shell to the total luminosity would be smaller than for a model with only an H burning shell. So, this shell would be thinner and removed outward.

But the fraction of the total mass occupied by the H burning shell is only in the

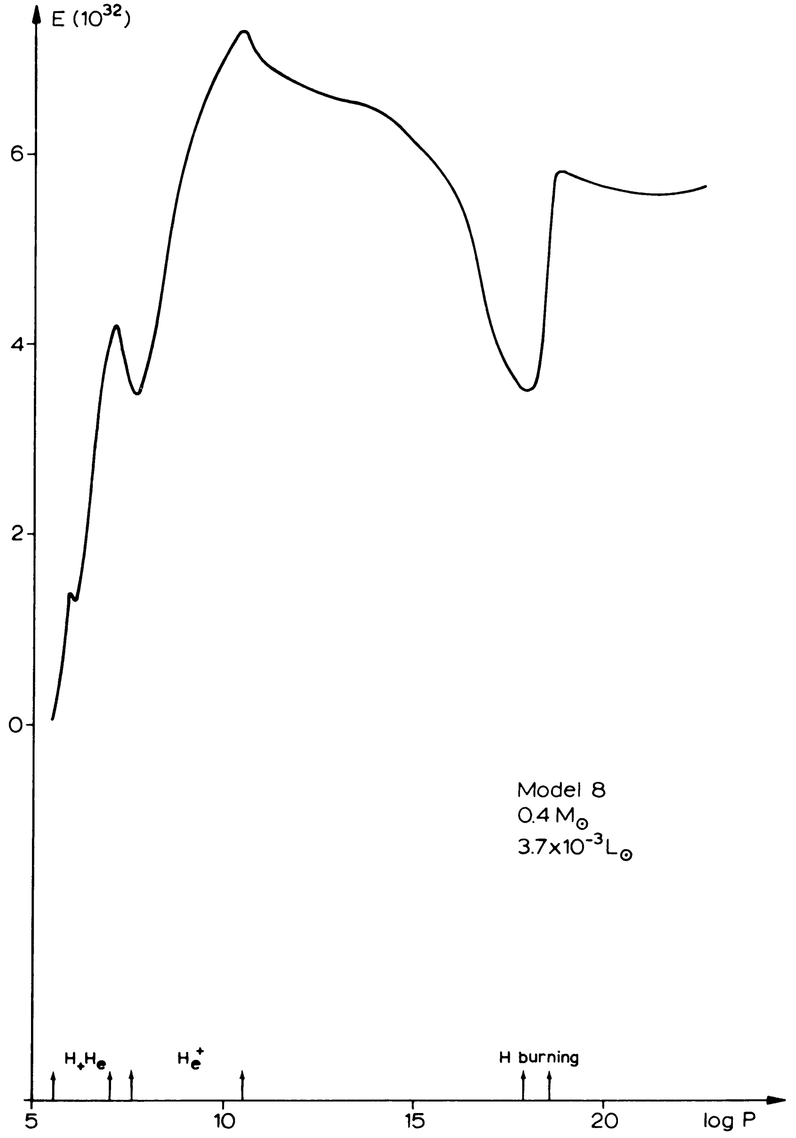


Fig. 4. The energy integral vs the pressure in the model 8.

https://doi.org/10.1017/S0074180900097205 Published online by Cambridge University Press

range of $10^{-4}$–$10^{-5}$. The modification of both the locus and the width of this shell would not change the structure of the envelope which surrounds it. So the overall structure of the models would not be modified.

## 5. Conclusion

It could be expected that models of white dwarfs with an energy source located near the surface would be vibrationally unstable (Ledoux *et al.*, 1950; Baglin, 1967).

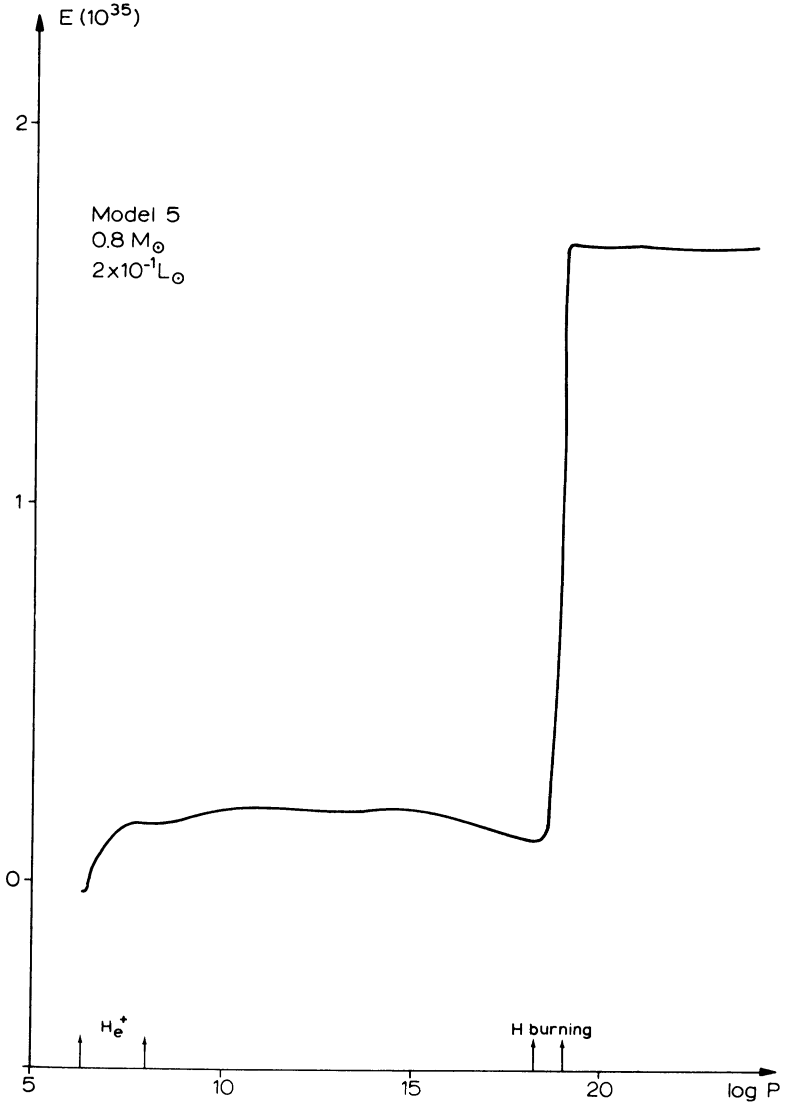


Fig. 5. The energy integral vs the logarithm of the pressure in the model 5.

https://doi.org/10.1017/S0074180900097205 Published online by Cambridge University Press

Our preliminary results* show that, in fact, we find a region in the H – R diagram where the $x$-mechanism is mainly responsible for the instability.

It is interesting to notice that the two models which present this type of instability are located in the prolongation of the instability strip of the Cepheids (Christy, 1970) (Figure 6).

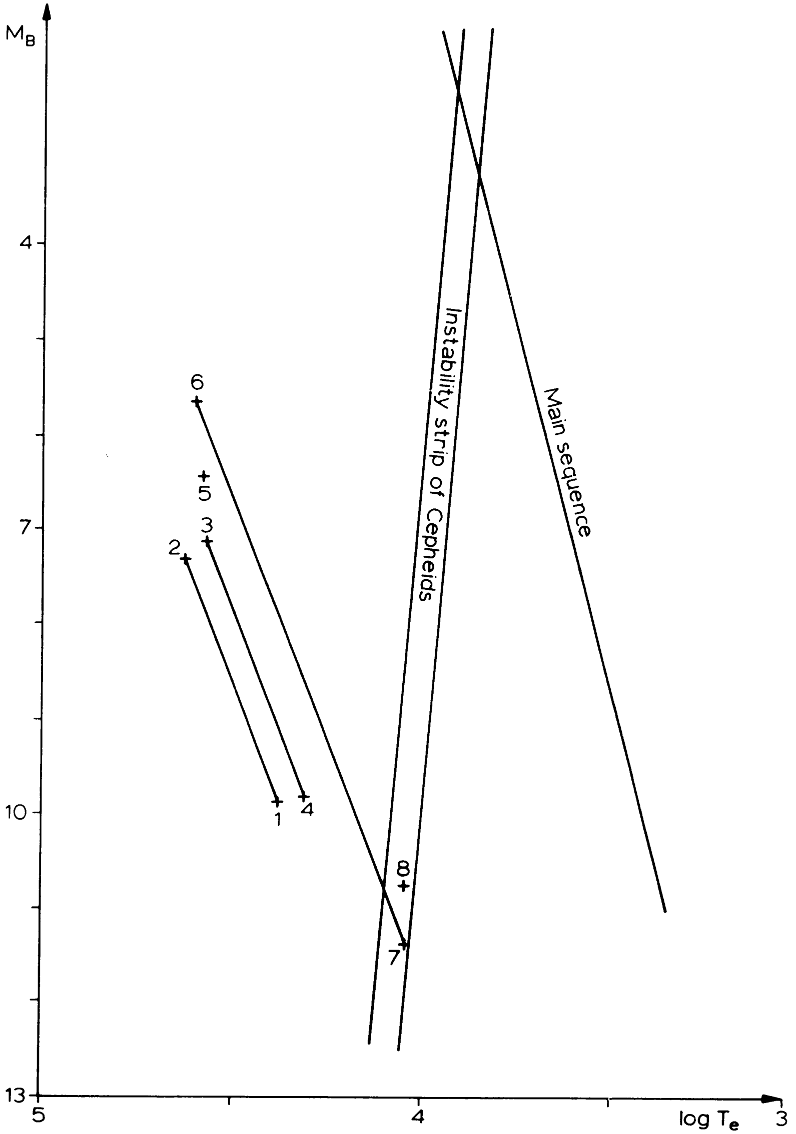


Fig. 6. H – R diagram. Our models are located by a cross and their number as in Table I. The main sequence is given by Morton and Adams (1968) and the instability strip of the Cepheids by Christy (1970). Straight lines are drawn between models of same mass.

* More detailed results will be published later.

Variable white dwarfs can exist but they must be very difficult to observe. The amplitudes of the pulsations are very small; for a typical Cepheid, the amplitude of the luminosity variation is of the order of 1 mag; it decreases to $\frac{1}{100}$ of magnitude for $\delta$ Scuti variables; for white dwarf variables it must be less than $\frac{1}{100}$ of magnitude. On the other hand, the amplification rates found for our models are very long (Table III).

## References

Baglin, A.: 1967, *Ann. Astrophys.* **30**, 617.
Chandrasekhar, S.: 1939, *An Introduction to Stellar Structure*, Ed. Dover.
Christy, R. F.:1970, *R.A.S.C.J.* **64**, 8.
Cohen, J. M., Lapidus, A. H., and Cameron, A. G. W.: 1969, *Astrophys. Space Sci.* **5**, 113.
Harper, R. R. and Rose, W. K.: 1969, preprint.
Hubbard, W. B. and Wagner, R. L.: 1970, *Astrophys. J.* **159**, 93.
Lauterborn, D.: 1970, *Astron. Astrophys.* **7**, 150.
Ledoux, P. J. and Sauvenier-Goffin, E.: 1950, *Astrophys. J.* **111**, 611.
Ledoux, P. J. and Walraven, T.: 1958, *Handbuch der Physik* **LI**, Springer-Verlag, Berlin.
Morton, D. C. and Adams, T. F.: *Astrophys. J.* **151**, 614.
Ostriker, J. P. and Tassoul, J. L.: 1969, *Astrophys. J.* **155**, 987.
Salpeter, E. E.: 1961, *Astrophys. J.* **134**, 669.
Schatzman, E.: 1952, *Ann. Astrophys.* **15**, 361.
Van Horn, H. M.: 1970, *Astrophys. J.* **160**, L53.
Vila, S. C.: 1966, *Astrophys. J.* **146**, 437.
Vila, S. C.: 1967, *Astrophys. J.* **149**, 613.